Synergistic Toxicity of ZnO Nanoparticles and Dimethoate in Mice: Enhancing Their Biodistribution by Synergistic Binding of Serum Albumin and Dimethoate to ZnO Nanoparticles

Xincheng Yan, Xiaolong Xu, Mingchun Guo, Shasha Wang, Shang Gao, Shanshan Zhu, Rui Rong

Department of Chemistry, University of Science and Technology of China, Hefei 230026, People's Republic of China

Received 31 December 2015; revised 23 June 2016; accepted 2 July 2016

ABSTRACT: The extensive applications of ZnO nanoparticles (nano ZnO) and dimethoate (DM) have increased the risk of humans' co-exposure to nano ZnO and DM. Here, we report the synergistic effect of nano ZnO and DM on their biodistribution and subacute toxicity in mice. Nano ZnO and DM had a synergistic toxicity in mice. In contrast, bulk ZnO and DM did not cause an obvious synergistic toxicity in mice. Although nano ZnO was low toxic to mice, coexposure to nano ZnO and DM significantly enhanced DM-induced oxidative damage in the liver. Coadministration of nano ZnO with DM significantly increased Zn accumulation by 30.9 ± 1.9% and DM accumulation by 45.6 ± 2.2% in the liver, respectively. The increased accumulations of DM and Zn in the liver reduced its cholinesterase activity from 5.65 ± 0.32 to 4.37 ± 0.49 U/mg protein and induced hepatic oxidative stress. Nano ZnO had 3-fold or 2.4-fold higher binding capability for serum albumin or DM, respectively, than bulk ZnO. In addition, serum albumin significantly increased the binding capability of nano ZnO for DM by approximately four times via the interaction of serum albumin and DM. The uptake of serum albumin- and DM-bound nano ZnO by the macrophages significantly increased DM accumulation in mice. Serum albumins play an important role in the synergistic toxicity of nano ZnO and DM. Environ Toxicol 32: 1202–1212, 2017.
Keywords: ZnO nanoparticles; dimethoate; oxidative stress; synergistic toxicity; serum albumin

INTRODUCTION

ZnO nanoparticles (nano ZnO) are one of the most abundantly used nanomaterials in sunscreens and cosmetics because of their efficient UV absorption properties (Kocbek et al., 2010; Ma et al., 2013). Nano ZnO is also widely utilized in commercial products, including toothpaste, pigments, medicine, drug carriers, and bioimaging probes (Zhang and Liu, 2010; Liu et al., 2011; Ng et al., 2011). In addition, nano ZnO is commonly used in the food industry as food additives, dietary supplements and food packaging components due to its antimicrobial property (Sharma et al., 2012a; Liu et al., 2015). Humans have a higher chance of being exposed to nano ZnO in food-related products than other nanoparticles (Cho et al., 2013). Currently, several cosmetics and food additives containing nano ZnO are actually on the market (Rashidi and Khosravi-Darani, 2011). Nano ZnO is also being explored for its potential use as fungicide in agriculture (He et al., 2011). The widespread application of nano ZnO increases the potential for their release to the

Additional Supporting Information may be found in the online version of this article.

Correspondence to: X. Xu; e-mail: Xuxl@ustc.edu.cn

Contract grant sponsor: National Natural Science Foundation of China.

Contract grant numbers: 21171157, 20871111, and 20571069.

Published online 21 July 2016 in Wiley Online Library (wileyonlinelibrary.com). DOI: 10.1002/tox.22317

environment, which has raised public concerns about their adverse effects on human health (Kumari et al., 2011; Sharma et al., 2012b; Zhao et al., 2013). Previous studies have shown that nano ZnO has relative high toxicity to different biological systems (Adam et al., 2014; Ma et al., 2014).

Dimethoate (DM), one of the most popular organophosphorus insecticides, is frequently used against a wide range of insects in agriculture and for housefly control due to its high effectiveness (Priya et al., 2011; Ayed-Boussema et al., 2012; Guo et al., 2012). The residue of DM and its analog have been found in soil, crops, water, and foods, including cow's milk (Amara et al., 2011; Soler et al., 2011; Feng et al., 2012). The main toxic effect of DM is the inhibition of cholinesterase (ChE), which causes dysfunction at the neuromuscular junction and blocks the nerve conduction (Augustyniak et al., 2007; Karalliedde, 1999). In addition, as a lipophilic molecule, DM can interact favorably with the cell membrane and easily pass through the cell membrane into the cytoplasm (Amara et al., 2012). Once inside the cell, DM can induce the production of reactive oxygen species, which in turn generates oxidative stress in tissues (Sharma et al. 2005a,b; Mahjoubi-Samet et al., 2008; Amara et al., 2012).

The extensive applications of both nano ZnO and DM have increased the risk of humans' coexposure to nano ZnO and DM. For example, in some developing countries, most of the houses in rural, less developed regions do not have piped water. Some farmers drink the natural water and cow's milk and eat the fruits and vegetables. The natural water, fruits, cow's milk, and vegetables may contaminate with DM residue and nano ZnO. In addition, some farmers may eat the foods that contain nano ZnO additive. It is necessary to identify the combined effect of co-exposure to nano ZnO and DM on human health. Our recent studies revealed that both nano and bulk ZnO have nearly identical enhanced effects on DM-induced toxicity in mice by oral administration due to that both nano and bulk ZnO dissolve quickly in acidic gastric fluid (Yan et al., 2015). In this study, in order to analyze the mechanism of combined toxicity of nano ZnO and DM and the effect of the size of nano ZnO on their combined toxicity, we have determined the biodistribution, serum biochemical parameters, oxidative stress makers, and histopathological changes in mice via intraperitoneal administration of nano or bulk ZnO and/or DM. In addition, the binding of bovine serum albumin (BSA) and DM to nano or bulk ZnO was investigated *in vitro*. The results show that the size of nano ZnO has a marked effect on their combined toxicity of nano ZnO and DM and demonstrate that serum albumins play an important role in their combined toxicity.

MATERIALS AND METHODS

Chemicals

Nano ZnO and bulk ZnO used in our experiments are commercially available from Sigma Chemical Co. (St. Louis, MO) and characterized by transmission electron microscopy (TEM) (JEM-2010; JEOL, Tokyo, Japan) and Zetasizer (3000HSA/Nano-ZS; Malvern, Malvern, UK), respectively. DM (99.3%, batch no, 40606) was purchased from Aladdin Chemistry Co. (Shanghai, China). Nano or bulk ZnO and DM were suspended in 0.15 M NaCl before the injection into mice.

Animals and Treatment

Male Kunming mice (20 ± 2 g, 6–8 weeks old) were purchased from the Animal Center of Anhui Medical University (Anhui, China). Animals were housed in stainless steel cages in a ventilated animal room under controlled conventional conditions (temperature 20 ± 2°C; relative humidity 60 ± 5%; 12 hours light/dark cycle). Distilled water and sterilized food for mice were available ad libitum. They were acclimated to this environment for seven days prior to dosing. All experiments were conducted in accordance with the guidelines of University of Science and Technology of China for the care and use of laboratory animals and with approval of the Animal Ethical Committee of University of Science and Technology of China. Mice were randomly divided into six groups with 10 male mice in each group: control group (treated with physiological saline) and five experimental groups (20 mg/kg BW nano ZnO, 20 mg/kg BW bulk ZnO, 10 mg/kg BW DM, 20 mg/kg BW nano ZnO + 10 mg/kg BW DM, and 20 mg/kg BW bulk ZnO + 10 mg/kg BW DM). Chemicals were administered to mice via intraperitoneal injection at a dose of 0.1 mL/10 g BW, respectively, once a day for 14 consecutive days. After 14 days, blood samples were collected from the tail vein after being anaesthetized by ether. Serum was harvested by centrifuging blood at 3000 rpm for 10 minutes. The tissues and organs, such as the heart, liver, spleen, lung, kidney, and brain, were excised, washed thoroughly with physiological saline, and weighed. The coefficients of organs to body weight were calculated as the ratio of organs (wet weight, mg) to body weight (g).

Serum Biochemical Parameters Assay

Liver function was evaluated with serum levels of aspartate aminotransferase (AST), alanine aminotransferase (ALT), alkaline phosphatase (ALP), lactate dehydrogenase (LDH), total bilirubin (TBIL), albumin protein (ALB), albumin/globulin (A/G), and total protein (TP). Nephrotoxicity was determined with creatinine (CRE) and blood urea nitrogen (BUN). All biochemical parameters were determined by an automatic biochemical analyzer (Roche Modular DPP System, Augsburg, Germany) using the commercial kits (Roche Diagnostics, Mannheim, Germany).

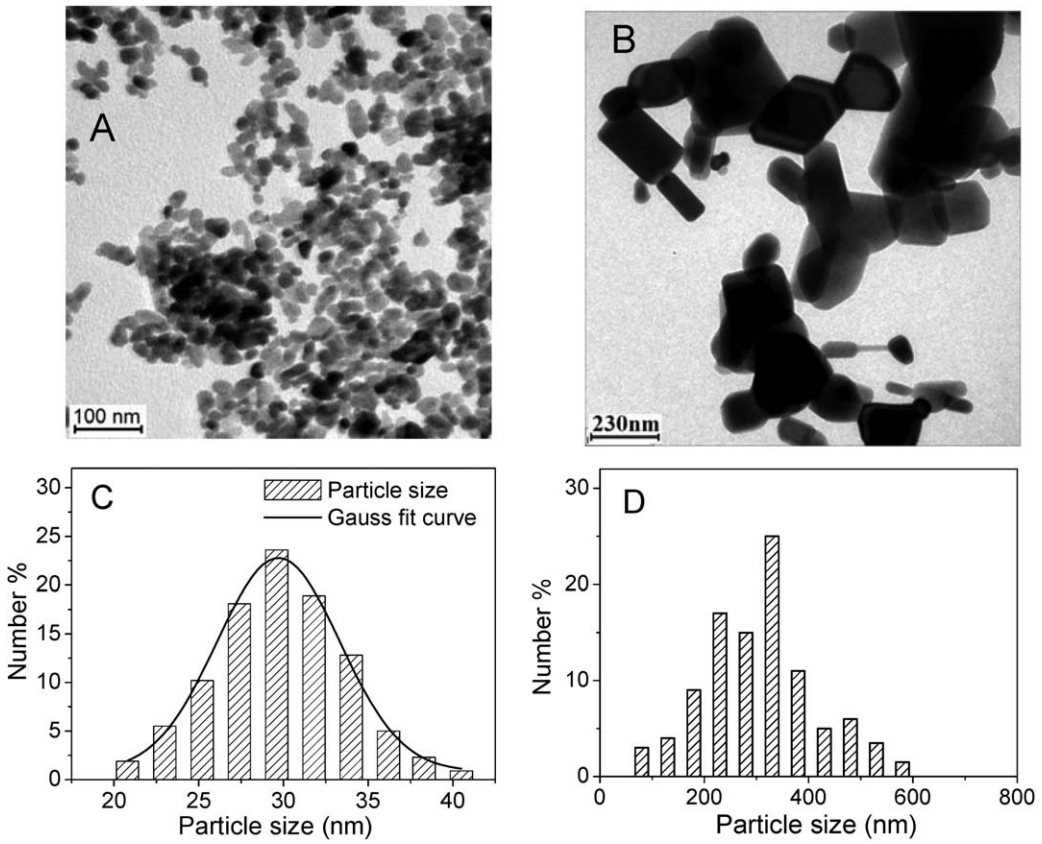

Fig. 1. TEM images of nano ZnO (A) and bulk ZnO (B). Size distribution profiles of nano ZnO (C) and bulk ZnO (D).

Histopathological Examination

All histopathological tests were performed using standard laboratory procedures. Tissues of the liver, kidney, heart, lung, spleen, and brain were cut out and immediately fixed in 10% (v/v) formalin, embedded in paraffin blocks, then sliced into 5 μm in thickness and placed onto glass slides. After hematoxylin and eosin staining, the slides were observed, and the photos were taken using an optical microscope (IX-81; Olympus, Japan) at 40× magnification. The identity and analysis of the pathology slides were blind to the pathologist.

Measurement of Oxidative Stress Makers

The activities of glutathione peroxide (GSH-Px), catalase (CAT), superoxide dismutase (SOD), and the level of lipid peroxidation product malondialdehyde (MDA) were determined using the commercial kits (Nanjing Jiancheng Bioeng Institute, Jiangsu, China), according to the manufacturer's instructions. After mice were sacrificed, ~0.1–0.3 g fresh liver tissue was excised and weighed accurately. The 1:9 (w/v) volume of 0.86% ice-cold saline was added, and the mixture was homogenized in an ice bath. The homogenate was centrifuged at 3000 rpm for 10 minutes at 4°C. The supernatant was collected and assayed for the oxidative biomarkers.

Measurement of ChE Activity

ChE activity was determined in liver tissue by the hydroxylamine-ferric chloride method using acetylcholine as a substrate (Hestrin, 1949). The rate of hydrolysis of acetylcholine was determined through the measurement of the remaining acetylcholine after hydrolysis catalyzed by ChE. The remaining acetylcholine reacted with hydroxylamine to form acethydroxamic acid which reacted with Fe^{3+} to produce the purple-brown color ferric-acethydroxamic acid compound, which could be spectrophotometrically determined at 520 nm. ChE activity was expressed as U/mg protein. One unit of enzyme is the amount of protein that decomposes 1 μmol of acetylcholine per minute at 37°C.

Analysis of Biodistributions of Zn and DM

The liver, kidney, heart, lung, spleen, or brain tissue (0.1–0.2 g) was digested with ultrapure HNO_3 solution for 12 hours. The solutions were then mixed with 0.5 mL H_2O_2 and heated at 130°C to remove the remaining HNO_3. The remaining solutions were diluted to 5 mL with 2% (v/v) HNO_3. The Zn contents in the solutions were measured by inductively coupled plasma-atomic emission spectrometry (ICP-AES) (Optima 7300 DV; PerkinElmer Corporation, Waltham, MA). The DM contents in the organs were

analyzed by gas chromatography−mass spectrometry (GC–MS) using the modified method described by Raposo et al. (2010). The liver, kidney, heart, lung, spleen, or brain tissue (0.1–0.2 g) was homogenized. The homogenates were centrifuged at 4000 rpm for 20 minutes at 4°C. The supernatant was added to a CNWBOND C18 SPE column (ANPEL Scientific Instrument Co., Shanghai, China), previously conditioned with 10 mL of methanol and 10 mL of water. The sample was allowed to pass through the column by gravity. The column was washed with 10 mL of 5% methanol in water and dried under vacuum for 20 minutes. The analyte was eluted with 10 mL methanol. The eluate was evaporated to dryness under a gentle stream of nitrogen at 25°C. The dry extract was dissolved in 50 μL of methanol, and 1 μL of the solution was injected into a Thermo Trace GC–ISQ MS system (Thermo Fisher Scientific, Waltham, MA) with a Thermo TR-5 MS capillary column (30 m × 0.25 mm).

Analysis of *In Vitro* Binding of BSA and DM to Nano or Bulk ZnO

A total of 50 mg nano or bulk ZnO was incubated with 5 mL of 0.15 M NaCl in 20 mM Tris-HCl (pH 7.4) containing 0.5 mg/mL BSA and/or 0.1 mg/mL DM at 4°C for 30 minutes. BSA- and/or DM-bound ZnO was separated from the mixture by centrifugation at 12,000 rpm for 10 minutes at 4°C. The ultraviolet absorbance of the supernatant was determined at 280 nm. The content of DM in each supernatant was measured using the GC–MS assay as described earlier.

Statistical Analysis

Results were expressed as mean ± SD ($n = 10$). Data were analyzed by one-way analysis of variance test using SPSS 16.0 (SPSS Inc., Chicago, IL). The Dunnett's test was used to compare the differences between the experimental groups and the control group. The statistical significance for all tests was set at $p < 0.05$.

RESULTS AND DISCUSSION

Characterization of Nano ZnO and Bulk ZnO

The microstructures and particle sizes of nano ZnO and bulk ZnO were characterized by TEM. As shown in Figure 1, the particles of nano ZnO had an approximately spherical morphology and an average size of 29.5 ± 1.2 nm with unimodal distribution. The particles of bulk ZnO had an approximately rod morphology with different sizes ranging from 80 to 600 nm. The zeta potentials of nano ZnO and bulk ZnO in 20 mM Tris-HCl (pH 7.4) containing 0.15 M NaCl were 14.9 ± 0.8 and 12.2 ± 0.9 mV, respectively.

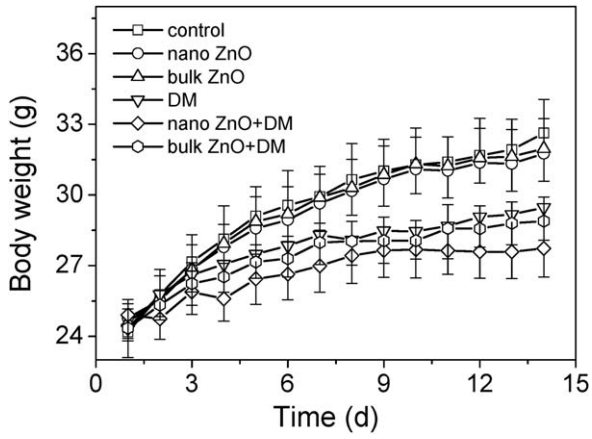

Fig. 2. Body weight changes of mice ($n = 10$) during exposure period. Physiological saline was used as control.

Effects of Coexposure on Body Weight Changes and Coefficients of Organs

During the entire exposure period, no abnormal daily activity and symptoms were observed in the control, nano ZnO, and bulk ZnO groups. A few signs of acute organophosphate poisoning including anorexia and reduced activity were observed in the DM and bulk ZnO + DM groups. The mice coexposure to nano ZnO and DM showed varying degrees of signs, such as loss of appetite, mild tremor, and piloerection. As shown in Figure 2, the body weights in the nano ZnO and bulk ZnO groups increased a little more slowly than the control group, whereas the body weight in the DM group increased much more slowly than the control group. Coexposure to nano ZnO and DM had a significant synergistic adverse effect on the weight gain. In contrast, coexposure to bulk ZnO and DM had no significant synergistic adverse effect on the weight gain. As shown in Table I, no significant changes were observed in the coefficients of the liver of the nano ZnO and bulk ZnO groups, compared with the control. In the DM group, the liver showed a significantly higher coefficient than the control group ($p < 0.05$). In the nano ZnO + DM group, the liver presented a significantly higher coefficient ($p < 0.05$) compared with all other three groups, indicating a synergistic effect of nano ZnO and DM on the liver coefficient. In contrast, coexposure to bulk ZnO and DM had no obvious synergistic effect on the liver coefficient. No significant changes were observed in the coefficients of the kidney, heart, lung, spleen, and brain of all exposure groups compared with the control.

Synergistic Effects on Biodistributions of Zn and DM

The biodistributions of Zn and DM were studied by ICP-AES and GC–MS, respectively, after exposure to nano or bulk ZnO and/or DM. As shown in Figure 3(A), major percentage of injected nano ZnO or bulk ZnO accumulated in

TABLE I. The coefficients of major organs of mice

Index	Control	Nano ZnO	Bulk ZnO	DM	Nano ZnO + DM	Bulk ZnO + DM
Liver/BW (mg/g)	53.9 ± 2.1	56.6 ± 1.7	54.9 ± 1.3	59.9 ± 1.2[a]	64.1 ± 4.3[a,d]	60.8 ± 2.2[a,d]
Kidney/BW (mg/g)	13.2 ± 0.7	13.7 ± 0.4	13.5 ± 0.7	13.6 ± 0.8	14.3 ± 0.4	13.8 ± 0.3
Heart/BW (mg/g)	4.63 ± 0.33	4.53 ± 0.38	4.58 ± 0.41	4.52 ± 0.22	4.51 ± 0.28	4.57 ± 0.38
Lung/BW (mg/g)	8.91 ± 0.32	9.01 ± 0.69	8.86 ± 0.29	8.55 ± 0.52	8.89 ± 0.45	8.94 ± 0.36
Spleen/BW (mg/g)	4.91 ± 0.93	4.88 ± 0.46	4.84 ± 0.45	4.73 ± 0.52	4.80 ± 0.49	4.90 ± 0.51
Brain/BW (mg/g)	19.8 ± 2.9	20.1 ± 1.0	20.2 ± 0.9	20.4 ± 0.9	20.2 ± 0.7	20.1 ± 0.6

The mice were intraperitoneally injected with nano or bulk ZnO and/or DM for 14 consecutive days. Physiological saline was used as control. Data were expressed as mean ± SD ($n = 10$).

[a] $p < 0.05$ *versus* the control.

[b] $p < 0.05$ *versus* the nano ZnO group.

[c] $p < 0.05$ *versus* the DM group.

[d] $p < 0.05$ *versus* the bulk ZnO.

the liver, kidney, and spleen. In the DM group, there were no significant changes in the Zn levels in all tested organs compared to the control group. In the nano ZnO + DM group, the Zn level was significantly higher in the liver than in the nano ZnO group ($p < 0.05$). This result indicates that coexposure to nano ZnO and DM significantly increases in the biodistribution density of Zn in the liver. However, coexposure to bulk ZnO and DM only slightly increased in the biodistribution density of Zn in the liver compared to the bulk ZnO group.

As shown in Figure 3(B), the major accumulation of DM occurred predominantly in the liver and kidney, and a slight accumulation of DM was found in the spleen and lung after injection of DM. Interestingly, in the nano ZnO + DM group, the DM levels in the liver and kidney were significantly higher than that in the DM group ($p < 0.05$), revealing that coexposure to nano ZnO and DM significantly increases the biodistribution densities of DM in the liver and kidney. In contrast, coexposure to bulk ZnO and DM only slightly increased the biodistribution densities of DM in the liver and kidney. These results taken together indicate that coexposure to nano ZnO and DM has a synergistic effect on the biodistributions of Zn and DM in the liver.

Effects of Coexposure on Histopathological Changes in Tissues

Figure 4 shows the histopathological photomicrographs of the liver tissues. In the nano ZnO and bulk ZnO groups, no abnormalities were observed in the mice liver. In the DM or bulk ZnO + DM group, the infiltration of inflammatory cell was observed around the central vein. In the nano ZnO + DM group, the inflammatory infiltration and multiple spotty necrosis were found around the central vein. In addition, the fibrosis was induced on the liver surface. These results indicate that coexposure to nano ZnO and DM induces more histopathological damages in the liver than exposure to either nano ZnO or DM alone, which is attributed to the coexposure-induced increases in the accumulation of DM and Zn in the liver. As a result, the liver in the nano ZnO + DM group showed significantly higher coefficient than that in either nano ZnO or DM group. By contrast,

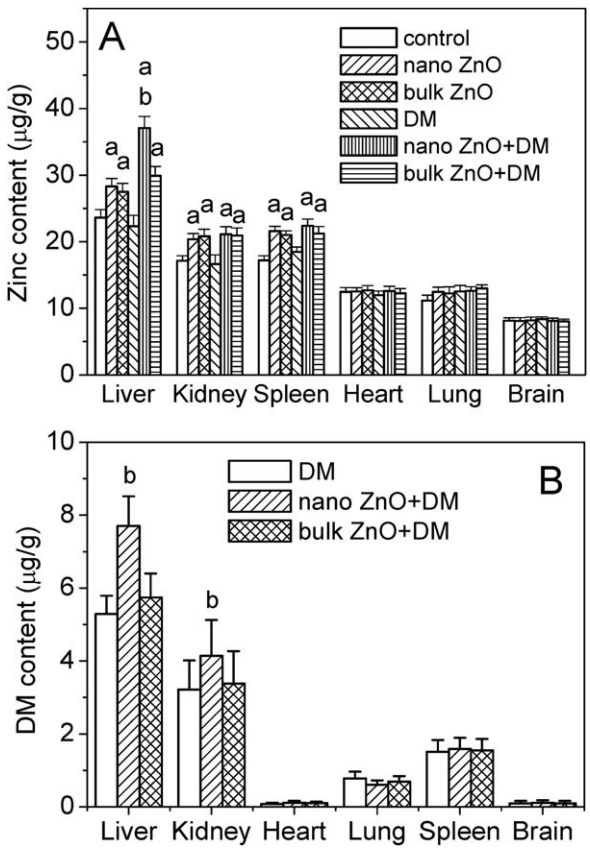

Fig. 3. Biodistributions of Zn and DM in different tissues of mice determined by ICP-AES and GC–MS. The mice were intraperitoneally injected with nano or bulk ZnO and/or DM for 14 consecutive days. (A) The contents of Zn in different tissues of mice. (B) The contents of DM in different tissues of mice. Physiological saline was used as control. [a] $p < 0.05$ *versus* the control; [b] $p < 0.05$ *versus* the nano ZnO (A) or DM (B) group. Values represent mean ± SD, $n = 10$.

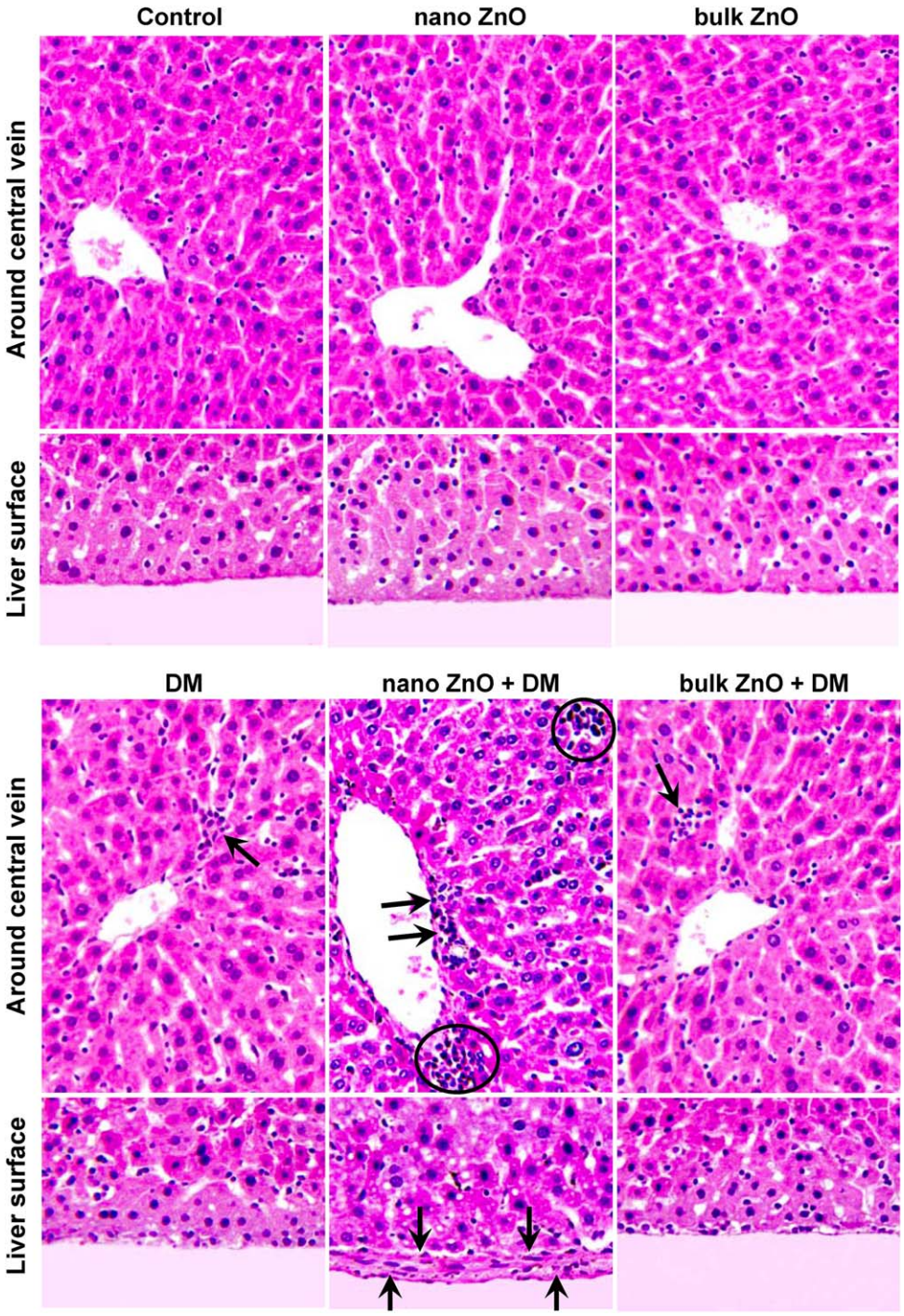

Fig. 4. Histopathological images of the liver tissue in mice following daily intraperitoneal injections of nano or bulk ZnO and/or DM for 14 days. No abnormalities were observed in the control, nano ZnO, and bulk ZnO groups. In the DM and bulk ZnO + DM groups, the infiltration of inflammatory cell (arrow) was seen around the central vein. In the nano ZnO + DM group, inflammatory infiltration (arrows) and multiple spotty necrosis (circles) around the central vein and the fibrosis (arrows) on the liver surface were induced. Physiological saline was used as control. [Color figure can be viewed at wileyonlinelibrary.com.]

coexposure to bulk ZnO and DM did not significantly increase DM-induced histopathological damages in the liver. No obvious abnormal pathological changes were found in the kidney, heart, lung, spleen, and brain tissues in all injected mice compared with the control group (Fig. S1).

TABLE II. Changes of biochemical parameters in serum of mice

Index	Control	Nano ZnO	Bulk ZnO	DM	Nano ZnO + DM	Bulk ZnO + DM
AST (U/L)	101 ± 14	124 ± 10	107 ± 8.9	149 ± 16[a]	174 ± 15[a,c]	163 ± 11[a,d]
ALT (U/L)	37.6 ± 3.4	45.2 ± 13.8	41.3 ± 9.4	60.6 ± 17.2[a]	82.4 ± 14.9[a,c]	70.5 ± 12.4[a,d]
ALP (U/L)	118 ± 19	145 ± 18	131 ± 16	195 ± 55[a]	298 ± 33[a,c]	223 ± 41[a,d]
LDH (U/L)	659 ± 34	844 ± 36[a]	785 ± 41[a]	903 ± 32[a]	1046 ± 43[a,c]	962 ± 52[a,d]
TBIL (μmol/L)	1.21 ± 0.18	1.24 ± 0.09	1.23 ± 0.06	1.18 ± 0.16	1.23 ± 0.12	1.23 ± 0.14
ALB (g/L)	34.2 ± 1.5	30.9 ± 2.4	31.4 ± 3.1	33.4 ± 1.7	22.5 ± 2.2[a,c]	29.8 ± 2.4
A/G	1.37 ± 0.05	1.24 ± 0.08	1.29 ± 0.09	1.31 ± 0.10	1.07 ± 0.12[a,c]	1.26 ± 0.08
TP (g/L)	59.3 ± 2.8	55.6 ± 4.3	57.9 ± 3.1	59.1 ± 4.2	43.8 ± 4.3[a,c]	53.9 ± 3.7
CRE (μmol/L)	61.6 ± 4.4	59.6 ± 3.6	60.7 ± 3.8	60.8 ± 3.9	60.7 ± 1.6	60.7 ± 2.4
BUN (mmol/L)	6.22 ± 0.72	6.36 ± 0.71	6.30 ± 0.56	6.53 ± 0.63	6.50 ± 0.79	6.50 ± 0.38

The mice were intraperitoneally injected with nano or bulk ZnO and/or DM for 14 consecutive days. Physiological saline was used as control. Data were expressed as mean ± SD ($n = 10$).

[a] $p < 0.05$ *versus* the control.

[b] $p < 0.05$ *versus* the nano ZnO group.

[c] $p < 0.05$ *versus* the DM group.

[d] $p < 0.05$ *versus* the bulk ZnO.

Effects of Coexposure on Serum Biochemical Parameters

The synergistic toxicity of nano ZnO and DM in mice was analyzed by blood biochemical assay. Table II shows the serum biochemical parameters in the mice after exposure to nano or bulk ZnO and/or DM. In the nano ZnO and bulk ZnO groups, there were no significant changes in all serum biochemical parameters compared with the control group, except that their LDH showed a significant increased level ($p < 0.05$), suggesting that exposure to nano ZnO or bulk ZnO only slightly affects on the liver function but does not affect on the kidney function. By contrast, the mice exposure to DM showed significant increases in AST, ALT, ALP, and LDH levels ($p < 0.05$) compared to the control group, indicating the liver dysfunction caused by DM. In the nano ZnO + DM group, the AST, ALT, ALP, and LDH levels significantly increased, and the ALB and TP levels and A/G ratio significantly decreased compared to the either nano ZnO or DM group ($p < 0.05$), suggesting that coexposure to nano ZnO and DM has a synergistic effect on the liver dysfunction. The significant increase in LDH level is attributed to hepatocellular necrosis. However, coexposure to bulk ZnO and DM did not significantly aggravate DM-induced liver dysfunction. No obvious changes were observed in kidney function markers CRE and BUN in all exposed mice, indicating that the renal function does not significantly affected by exposure to nano or bulk ZnO and/or DM.

Effects of Coexposure on ChE Activity of the Liver

The synergistic toxicity of nano ZnO and DM in mice was investigated by ChE assay. It has been reported that DM is a ChE inhibitor (Karalliedde, 1999; Sayim, 2007). Figure 5 shows the ChE activities in the liver of the mice after exposure to nano or bulk ZnO and/or DM. In the nano ZnO and bulk ZnO groups, there was no significant change in the ChE activity compared to the control group. The ChE activity was significantly inhibited in the liver of mice treated with DM compared to the control group ($p < 0.05$). In the nano ZnO + DM group, the ChE activity in the liver was significantly inhibited compared to the either nano ZnO or DM group ($p < 0.05$), suggesting that nano ZnO significantly enhances the inhibition of the ChE activity by DM, which is attributed to an increase in DM accumulation in the liver after coexposure to nano ZnO and DM. However, coexposure to bulk ZnO and DM did not significantly affect on the inhibition of the ChE activity by DM.

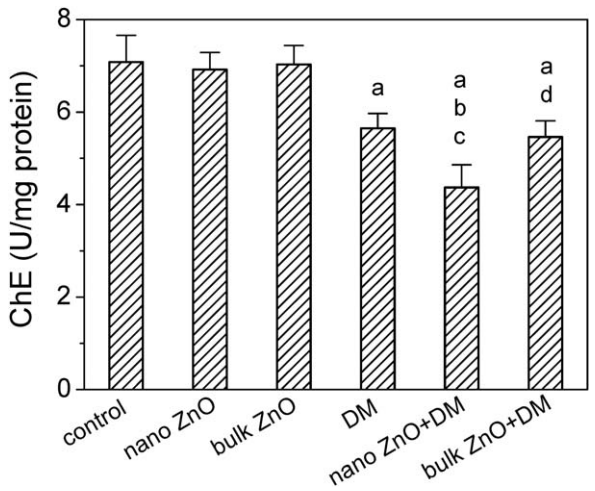

Fig. 5. The ChE activity of liver in mice following daily intraperitoneal injections of nano or bulk ZnO and/or DM for 14 consecutive days. Physiological saline was used as control. [a] $p < 0.05$ *versus* the control; [b] $p < 0.05$ *versus* the nano ZnO group; [c] $p < 0.05$ *versus* the DM group; [d] $p < 0.05$ *versus* the bulk ZnO. Values represent mean ± SD, $n = 10$.

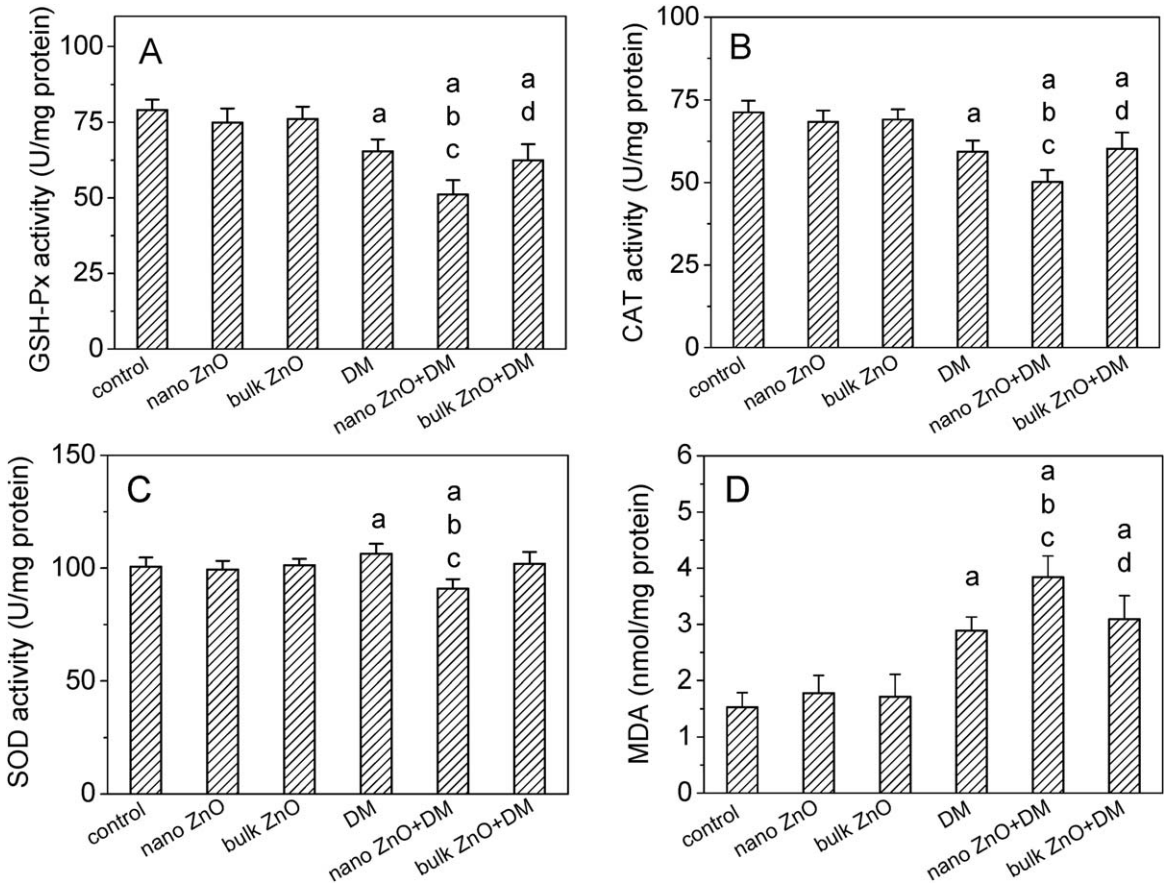

Fig. 6. The activities of antioxidative enzymes, GSH-Px, CAT, and SOD, and the MDA level of the liver of mice after intraperitoneal injection with nano or bulk ZnO and/or DM for 14 consecutive days. Physiological saline was used as control. [a]$p < 0.05$ *versus* the control; [b]$p < 0.05$ *versus* the nano ZnO group; [c]$p < 0.05$ *versus* the DM group; and [d]$p < 0.05$ *versus* the bulk ZnO. Values represent mean ± SD, $n = 10$.

Effects of Coexposure on Oxidative Damage in Tissues

The synergistic effect of cotreatment with nano ZnO and DM on the oxidative stress in the liver of mice was investigated by assaying the endogenous antioxidative enzymes, GSH-Px, CAT, and SOD. It was reported that decreased levels of antioxidative enzymes are associated to increased oxygen free radical production (Xu et al., 2010). As shown in Figure 6, exposure to nano ZnO or bulk ZnO did not cause obvious oxidative stress in the liver. By contrast, exposure to DM caused significant oxidative stress in the liver as indicated by the significant decreases in GSH-Px and CAT activities in the liver after exposure to DM. The oxidative stress is accounted for the high accumulation of DM in the liver after exposure to DM. It is worthwhile to note that exposure to DM caused an increase in SOD activity in the liver. The increased activity of SOD is accounted for an activation of the compensatory mechanism through the effects of DM on liver cells (Prakasam et al., 2001). Coexposure to nano ZnO and DM led to significant ($p < 0.05$) decreases in the GSH-Px, CAT, and SOD activities in the liver compared with the either nano ZnO or DM group, indicating that coexposure to nano ZnO and DM induces more severe oxidative stress in the liver than exposure to either nano ZnO or DM alone. However, coexposure to bulk ZnO and DM did not significantly affect on the DM-induced oxidative stress in the liver.

MDA is the product of lipid peroxidation, the level of which reflects the level of oxidative damage in tissues. As shown in Figure 6(D), exposure to nano ZnO did not cause a significant change in the MDA level in the liver, compared with the control. However, the MDA level in the liver significantly increased ($p < 0.05$) in the DM group compared with the control, indicating that DM-induced lipid peroxidation was produced in the liver. The oxidative stress in the liver resulted in its dysfunction (Table II) and histopathological changes (Fig. 4). Cotreatment with nano ZnO and DM resulted in significantly higher MDA concentration in the liver compared with the either nano ZnO or DM group ($p < 0.05$), suggesting a synergistic effect of nano ZnO and DM on the lipid peroxidation in the liver, which could be

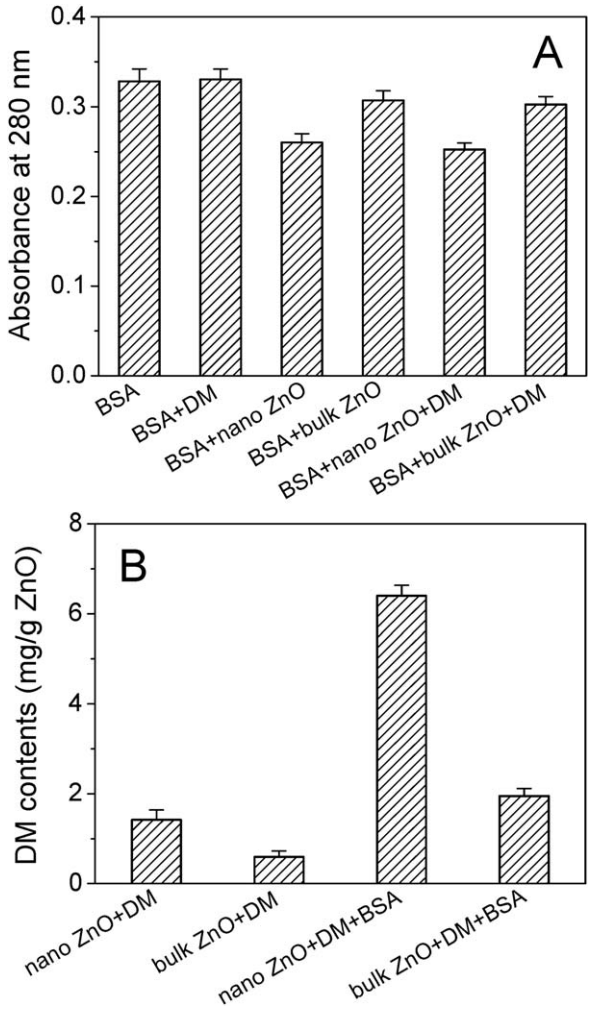

Fig. 7. *In vitro* binding of nano or bulk ZnO with BSA and DM. A total of 50 mg nano or bulk ZnO was incubated with 5 mL of 0.15 M NaCl in 20 mM Tris-HCl (pH 7.4) containing 0.5 mg/mL BSA and/or 0.1 mg/mL DM at 4°C for 30 minutes. Nano or bulk ZnO was separated from the mixture by centrifugation. (A) The ultraviolet absorbance of the supernatants. (B) The amount of DM bound on nano or bulk ZnO. Values represent mean ± SD, $n = 3$.

explained by the fact that nano ZnO and DM significantly enhanced the accumulation of each other in the liver. In contrast, coexposure to bulk ZnO and DM did not significantly affect on the DM-induced lipid peroxidation in the liver.

In Vitro Binding of BSA and DM to Nano and Bulk ZnO

When nano ZnO and DM are intraperitoneally administered, the nano ZnO and DM are absorbed into the portal circulation via the peritoneum (Guerrero et al., 2010). After entering blood, a variety of serum proteins including serum albumin bind to the surface of nano ZnO (Dembereldorj et al., 2012; Sasidharan et al. 2013). The serum protein-bound nano ZnOs are taken up by the macrophages in the organs, such as liver and kidney, and then detained in the organs. Serum albumin is the most abundant serum protein in blood plasma and serves as a versatile transporter for numerous endogenous compounds and drug molecules (Junk et al., 2011). In order to investigate the mechanism of a synergistic effect of coexposure to nano ZnO and DM on the biodistributions of Zn and DM in the liver, the binding of nano or bulk ZnO with BSA and DM was investigated *in vitro*. As shown in Figure 7(A), the ultraviolet absorbance of BSA solution at 280 nm did not change after incubation with DM. The ultraviolet absorbance of BSA solution at 280 nm decreased after incubation with nano ZnO or bulk ZnO, indicating the binding of BSA on nano ZnO or bulk ZnO. The binding capabilities of nano ZnO and bulk ZnO for BSA were calculated to be 10.5 ± 0.2 and 3.2 ± 0.1 mg/g, respectively. DM did not affect the binding capabilities of nano ZnO and bulk ZnO for BSA. As shown in Figure 7(B), the binding capabilities of nano ZnO and bulk ZnO for DM were 1.42 ± 0.11 and 0.59 ± 0.06 mg/g, respectively, in the absence of BSA. Interestingly, the binding capability of nano ZnO for DM dramatically increased from 1.42 ± 0.11 to 6.40 ± 0.12 mg/g in the presence of BSA. The binding capability of bulk ZnO for DM also increased from 0.59 ± 0.06 to 1.95 ± 0.08 mg/g in the presence of BSA. These results taken together indicate that nano ZnO has greater binding capability for either BSA or DM than bulk ZnO and that BSA significantly enhances the binding of DM to nano ZnO. Nano ZnO has a far larger surface area than bulk ZnO, which contributes to its greater binding capability for either BSA or DM than bulk ZnO.

The result of fluorescence titration of BSA with DM showed that DM can bind to BSA with an association constant of $(1.39 \pm 0.02) \times 10^2\ M^{-1}$ (Fig. S2). Serum albumin significantly increases the binding capability of nano ZnO for DM by approximately four times through the binding of DM-bound serum albumin to nano ZnO [Fig. 7(B)]. The uptake of serum albumin- and DM-bound nano ZnO by the macrophages in the liver results in a significant increase in the DM level in the organ. The enhancement of the binding of DM to nano ZnO by serum albumin accounts for that coexposure to nano ZnO and DM significantly increases in the biodistribution density of DM in the liver. Therefore, serum albumins play an important role in the synergistic accumulation of DM in mice.

The lipophilic nature of DM facilitates its interaction with the cell membrane and leads to perturbations in the phospholipids bilayer structure, which allows nano ZnO to easily pass through the membrane and distribute into the tissues (Amara et al., 2012). As a result, DM significantly increases in the biodistribution density of Zn in the liver. The synergistic accumulation of Zn and DM after coexposure to nano ZnO and DM contributes to their cooperative effect on their toxicity in mice.

However, coexposure to bulk ZnO and DM did not induce an obvious synergistic accumulation of Zn and DM in the liver. The ZnO surface area greatly affected its DM-binding capability. Bulk ZnO with small surface area demonstrated a significantly lower DM-binding capability than nano ZnO. In addition, the binding capability of bulk ZnO for DM was still much less than that of nano ZnO for DM in the presence of serum albumin. Therefore, the uptake of serum albumin- and DM-bound bulk ZnO by the macrophages in the liver after co-exposure to bulk ZnO and DM resulted in a slight increase in the DM level in the organ compared with exposure to DM alone. Because of its large size, it may be more difficult for bulk ZnO to penetrate through the cell membrane even in the presence of DM, compared with nano ZnO. As a result, coexposure to bulk ZnO and DM only caused a slight increase in the Zn level in the liver compared with exposure to bulk ZnO alone.

Our previous work showed that both nano and bulk ZnO have nearly identical enhanced effects on DM-induced toxicity in mice by oral administration (Yan et al., 2015). However, the present results indicate that nano ZnO and DM have a synergistic subacute toxicity in mice, while bulk ZnO and DM do not cause an obvious synergistic toxicity in mice. The different results are caused by the fact that nano and bulk ZnO have different stabilities in acidic gastric fluid (pH 1.5) and physiological solution (pH 7.4), respectively. Both nano ZnO and bulk ZnO dissolve quickly in acidic gastric fluid regardless of particle size; therefore, they have nearly identical enhanced effects on DM-induced toxicity in mice (Yan et al., 2015). In contrast, most of nano and bulk ZnO remain insoluble in physiological solution (pH 7.4) (Song et al., 2010; Shi et al., 2012; Seok et al., 2013). After intraperitoneal administration, nano or bulk ZnO are absorbed into the blood mainly in particulate forms. Nano ZnO with larger surface area has greater binding capability for BSA and DM than bulk ZnO, which contributes to significantly synergistic accumulation of DM and Zn in mice, while bulk ZnO and DM only cause slightly synergistic accumulation of DM and Zn in mice. As a result, nano ZnO and DM have a synergistic subacute toxicity in mice, while bulk ZnO and DM do not cause an obvious synergistic toxicity in mice. Therefore, the size of nano ZnO has a marked effect on their synergistic toxicity of nano ZnO and DM.

CONCLUSION

Nano ZnO and DM have a synergistic subacute toxicity in mice via intraperitoneal administration. Although nano ZnO at a dose of 20 mg/kg BW is low toxic to mice, coexposure to nano ZnO and DM significantly enhances DM-induced damage in the liver, which is attributed to the synergistic accumulation of Zn and DM in the liver. Serum albumin can significantly enhance the binding of DM to nano ZnO via the interaction of serum albumin and DM, which causes the significant increase in the DM accumulation in the liver. The enhanced accumulation of Zn and DM induces significant oxidative stress in the liver, which causes severe liver injury. Serum albumins play an important role in the synergistic toxicity of nano ZnO and DM. In contrast, bulk ZnO and DM do not cause an obvious synergistic toxicity in mice via intraperitoneal administration. These findings suggest that with the increasing use of nanomaterials, more attention should be paid to the synergistic adverse effects of coexposure to nanoparticles and other toxic substances on human health.

REFERENCES

Adam N, Leroux F, Knapen D, Bals S, Blust R. 2014. The uptake of ZnO and CuO nanoparticles in the water-flea Daphnia magna under acute exposure scenarios. Environ Pollut 194:130–137.

Amara IB, Soudani N, Troudi A, Bouaziz H, Boudawara T, Zeghal N. 2011. Antioxidant effect of vitamin E and selenium on hepatotoxicity induced by dimethoate in female adult rats. Ecotoxicol Environ Saf 74:811–819.

Amara IB, Soudani N, Troudi A, Hakim A, Zeghal KM, Boudawara T, Zeghal N. 2012. Dimethoate induced oxidative damage and histopathological changes in lung of adult rats: Modulatory effects of selenium and/or vitamin E. Biomed Environ Sci 25:340–351.

Augustyniak M, Migula P, Mesjasz-Przybylowicz J, Tarnawska M, Nakonieczny M, Babczynska A, Przybylowicz W, Augustyniak MG. 2007. Short-term effects of dimethoate on metabolic responses in *Chrysolina pardalina* (Chrysomelidae) feeding on *Berkheya coddii* (Asteraceae), a hyper-accumulator of nickel. Environ Pollut 150:218–224.

Ayed-Boussema I, Rjiba K, Moussa A, Mnasri N, Bacha H. 2012. Genotoxicity associated with oxidative damage in the liver and kidney of mice exposed to dimethoate subchronic intoxication. Environ Sci Pollut Res Int 19:458–466.

Cho WS, Kang BC, Lee JK, Jeong J, Che JH, Seok SH. 2013. Comparative absorption, distribution, and excretion of titanium dioxide and zinc oxide nanoparticles after repeated oral administration. Part Fibre Toxicol 10.

Dembereldorj U, Ganbold EO, Seo JH, Lee SY, Yang SI, Joo SW. 2012. Conformational changes of proteins adsorbed onto ZnO nanoparticle surfaces investigated by concentration-dependent infrared spectroscopy. Vib Spectrosc 59:23–28.

Feng Z, Sun X, Yang J, Hao D, Du L, Wang H, Xu W, Zhao X, Sun C. 2012. Metabonomics analysis of urine and plasma from rats given long-term and low-dose dimethoate by ultra-performance liquid chromatography-mass spectrometry. Chem Biol Interact 199:143–153.

Guerrero S, Araya E, Fiedler JL, Arias JI, Adura C, Albericio F, Giralt E, Arias JL, Fernandez MS, Kogan MJ. 2010. Improving the brain delivery of gold nanoparticles by conjugation with an amphipathic peptide. Nanomedicine 5:897–913.

Guo R, Ren X, Ren H. 2012. A new method for analysis of the toxicity of organophosphorus pesticide, dimethoate on rotifer based on response surface methodology. J Hazard Mater 237–238:270–276.

He L, Liu Y, Mustapha A, Lin M. 2011. Antifungal activity of zinc oxide nanoparticles against *Botrytis cinerea* and *Penicillium expansum*. Microbiol Res 166:207–215.

Hestrin S. 1949. The reaction of acetylcholine and other carboxylic acid derivatives with hydroxylamine, and its analytical application. J Biol Chem 180:249–261.

Junk MJ, Spiess HW, Hinderberger D. 2011. Characterization of the solution structure of human serum albumin loaded with a metal porphyrin and fatty acids. Biophys J 100:2293–2301.

Karalliedde L. 1999. Organophosphorus poisoning and anaesthesia. Anaesthesia 54:1073–1088.

Kocbek P, Teskac K, Kreft ME, Kristl J. 2010. Toxicological aspects of long-term treatment of keratinocytes with ZnO and TiO_2 nanoparticles. Small 6:1908–1917.

Kumari M, Khan SS, Pakrashi S, Mukherjee A, Chandrasekaran N. 2011. Cytogenetic and genotoxic effects of zinc oxide nanoparticles on root cells of *Allium cepa*. J Hazard Mater 190:613–621.

Liu HL, Yang HL, Lin BC, Zhang W, Tian L, Zhang HS, Xi ZG. 2015. Toxic effect comparison of three typical sterilization nanoparticles on oxidative stress and immune inflammation response in rats. Toxicol Res 4:486–493.

Liu Y, Ai K, Yuan Q, Lu L. 2011. Fluorescence-enhanced gadolinium-doped zinc oxide quantum dots for magnetic resonance and fluorescence imaging. Biomaterials 32:1185–1192.

Ma H, Williams PL, Diamond SA. 2013. Ecotoxicity of manufactured ZnO nanoparticles—A review. Environ Pollut 172:76–85.

Ma HB, Wallis LK, Diamond S, Li SB, Canas-Carrell J, Parra A. 2014. Impact of solar UV radiation on toxicity of ZnO nanoparticles through photocatalytic reactive oxygen species (ROS) generation and photo-induced dissolution. Environ Pollut 193: 165–172.

Mahjoubi-Samet A, Fetoui H, Zeghal N. 2008. Nephrotoxicity induced by dimethoate in adult rats and their suckling pups. Pestic Biochem Physiol 91:96–103.

Ng KW, Khoo SP, Heng BC, Setyawati MI, Tan EC, Zhao X, Xiong S, Fang W, Leong DT, Loo JS. 2011. The role of the tumor suppressor p53 pathway in the cellular DNA damage response to zinc oxide nanoparticles. Biomaterials 32:8218–8225.

Prakasam A, Sethupathy S, Lalitha S. 2001. Plasma and RBCs antioxidant status in occupational male pesticide sprayers. Clin Chim Acta 310:107–112.

Priya DN, Modak JM, Trebse P, Zabar R, Raichur AM. 2011. Photocatalytic degradation of dimethoate using LbL fabricated TiO_2/polymer hybrid films. J Hazard Mater 195:214–222.

Raposo R, Barroso M, Fonseca S, Costa S, Queiroz JA, Gallardo E, Dias M. 2010. Determination of eight selected organophosphorus insecticides in postmortem blood samples using solid-phase extraction and gas chromatography/mass spectrometry. Rapid Commun Mass Spectrom 24:3187–3194.

Rashidi L, Khosravi-Darani K. 2011. The applications of nanotechnology in food industry. Crit Rev Food Sci Nutr 51:723–730.

Sasidharan NP, Chandran P, Sudheer Khan S. 2013. Interaction of colloidal zinc oxide nanoparticles with bovine serum albumin and its adsorption isotherms and kinetics. Colloids Surf B: Biointerfaces 102:195-–201.

Sayim F. 2007. Dimethoate-induced biochemical and histopathological changes in the liver of rats. Exp Toxicol Pathol 59:237–243.

Seok SH, Cho WS, Park JS, Na Y, Jang A, Kim H, Cho Y, Kim T, You JR, Ko S, Kang BC, Lee JK, Jeong J, Che JH. 2013. Rat pancreatitis produced by 13-week administration of zinc oxide nanoparticles: Biopersistence of nanoparticles and possible solutions. J Appl Toxicol 33:1089–1096.

Sharma V, Anderson D, Dhawan A. 2012a. Zinc oxide nanoparticles induce oxidative DNA damage and ROS-triggered mitochondria mediated apoptosis in human liver cells (HepG2). Apoptosis 17:852–870.

Sharma V, Singh P, Pandey AK, Dhawan A. 2012b. Induction of oxidative stress, DNA damage and apoptosis in mouse liver after sub-acute oral exposure to zinc oxide nanoparticles. Mutat Res Genet Toxicol Environ Mutagen 745:84–91.

Sharma Y, Bashir S, Irshad M, Gupta SD, Dogra TD. 2005a. Effects of acute dimethoate administration on antioxidant status of liver and brain of experimental rats. Toxicology 206:49-–57.

Sharma Y, Bashir S, Irshad M, Nag TC, Dogra TD. 2005b. Dimethoate-induced effects on antioxidant status of liver and brain of rats following subchronic exposure. Toxicology 215: 173–181.

Shi JW, Karlsson HL, Johansson K, Gogvadze V, Xiao LS, Li JT, Burks T, Garcia-Bennett A, Uheida A, Muhammed M, Mathur S, Morgenstern R, Kagan VE, Fadeel B. 2012. Microsomal glutathione transferase 1 protects against toxicity induced by silica nanoparticles but not by zinc oxide nanoparticles. ACS Nano 6: 1925–1938.

Soler J, Santos-Juanes L, Miro P, Vicente R, Arques A, Amat AM. 2011. Effect of organic species on the solar detoxification of water polluted with pesticides. J Hazard Mater 188:181–187.

Song W, Zhang J, Guo J, Ding F, Li L, Sun Z. 2010. Role of the dissolved zinc ion and reactive oxygen species in cytotoxicity of ZnO nanoparticles. Toxicol Lett 199:389–397.

Xu B, Xu ZF, Deng Y, Yang JH. 2010. Protective effects of chlorpromazine and verapamil against cadmium-induced kidney damage in vivo. Exp Toxicol Pathol 62:27–34.

Yan XC, Rong R, Zhu SS, Guo MC, Gao S, Wang SS, Xu XL. 2015. Effects of ZnO nanoparticles on dimethoate-induced toxicity in mice. J Agric Food Chem 63:8292–8298.

Zhang P, Liu W. 2010. ZnO QD@PMAA-co-PDMAEMA nonviral vector for plasmid DNA delivery and bioimaging. Biomaterials 31:3087–3094.

Zhao L, Sun Y, Hernandez-Viezcas JA, Servin AD, Hong J, Niu G, Peralta-Videa JR, Duarte-Gardea M, Gardea-Torresdey JL. 2013. Influence of CeO2 and ZnO nanoparticles on cucumber physiological markers and bioaccumulation of Ce and Zn: A life cycle study. J Agric Food Chem 61:11945–11951.